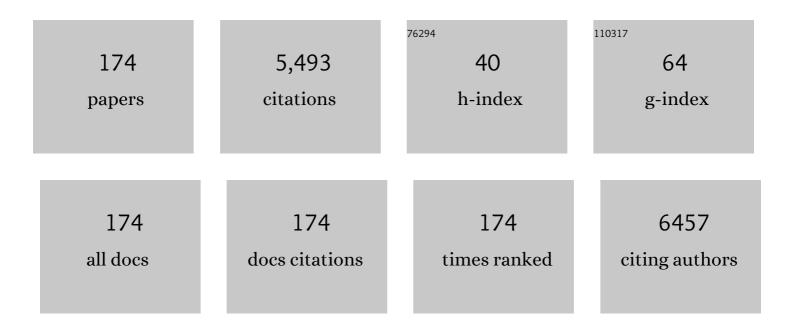


List of Publications by Year in descending order

Source: https://exaly.com/author-pdf/3474969/publications.pdf Version: 2024-02-01



#	Article	IF	CITATIONS
1	Ultrahigh-Loading of Ir Single Atoms on NiO Matrix to Dramatically Enhance Oxygen Evolution Reaction. Journal of the American Chemical Society, 2020, 142, 7425-7433.	6.6	430
2	Visible light driven selective oxidation of amines to imines with BiOCI: Does oxygen vacancy concentration matter?. Applied Catalysis B: Environmental, 2018, 228, 87-96.	10.8	237
3	Few-layer transition metal dichalcogenides (MoS2, WS2, and WSe2) for water splitting and degradation of organic pollutants: Understanding the piezocatalytic effect. Nano Energy, 2019, 66, 104083.	8.2	181
4	Single Iridium Atom Doped Ni ₂ P Catalyst for Optimal Oxygen Evolution. Journal of the American Chemical Society, 2021, 143, 13605-13615.	6.6	162
5	Boosting the oxygen evolution reaction using defect-rich ultra-thin ruthenium oxide nanosheets in acidic media. Energy and Environmental Science, 2020, 13, 5143-5151.	15.6	159
6	Defective/graphitic synergy in a heteroatom-interlinked-triggered metal-free electrocatalyst for high-performance rechargeable zinc–air batteries. Journal of Materials Chemistry A, 2021, 9, 18222-18230.	5.2	135
7	Synthesis of Spheres with Complex Structures Using Hollow Latex Cages as Templates. Advanced Functional Materials, 2005, 15, 1523-1528.	7.8	121
8	Rational Design Principles of the Quantum Anomalous Hall Effect in Superlatticelike Magnetic Topological Insulators. Physical Review Letters, 2019, 123, 096401.	2.9	104
9	Facile synthesis of SnO2 hierarchical porous nanosheets from graphene oxide sacrificial scaffolds for high-performance gas sensors. Sensors and Actuators B: Chemical, 2018, 258, 492-500.	4.0	89
10	One-dimensional phosphorus chain and two-dimensional blue phosphorene grown on Au(111) by molecular-beam epitaxy. Physical Review Materials, 2017, 1, .	0.9	89
11	The nucleation and growth of borophene on the Ag (111) surface. Nano Research, 2016, 9, 2616-2622.	5.8	86
12	Symmetry-Protected Ideal Type-II Weyl Phonons in CdTe. Physical Review Letters, 2019, 123, 065501.	2.9	86
13	Symmetry-Protected Topological Triangular Weyl Complex. Physical Review Letters, 2020, 124, 105303.	2.9	78
14	Photo-induced dye-sensitized BiPO4/BiOCl system for stably treating persistent organic pollutants. Applied Catalysis B: Environmental, 2021, 285, 119841.	10.8	73
15	Structural and electronic properties of ZnO nanotubes from density functional calculations. Nanotechnology, 2007, 18, 485713.	1.3	72
16	Single Fe atoms anchored by short-range ordered nanographene boost oxygen reduction reaction in acidic media. Nano Energy, 2019, 66, 104164.	8.2	68
17	Axial Modification of Cobalt Complexes on Heterogeneous Surface with Enhanced Electron Transfer for Carbon Dioxide Reduction. Angewandte Chemie - International Edition, 2020, 59, 19162-19167.	7.2	64
18	Tuning the electronic and magnetic properties of zigzag silicene nanoribbons by edge hydrogenation and doping. RSC Advances, 2013, 3, 24075.	1.7	63

#	Article	IF	CITATIONS
19	An essential descriptor for the oxygen evolution reaction on reducible metal oxide surfaces. Chemical Science, 2019, 10, 3340-3345.	3.7	63
20	Enhanced visible-light-driven photocatalytic hydrogen generation using NiCo2S4/CdS nanocomposites. Chemical Engineering Journal, 2019, 378, 122089.	6.6	59
21	First-principles calculations of reconstructed [0001] ZnO nanowires. Physical Review B, 2007, 76, .	1.1	58
22	The prediction of a family group of two-dimensional node-line semimetals. Nanoscale, 2017, 9, 13112-13118.	2.8	58
23	Three-Dimensional Dirac Phonons with Inversion Symmetry. Physical Review Letters, 2021, 126, 185301.	2.9	58
24	Defects-engineered tailoring of tri-doped interlinked metal-free bifunctional catalyst with lower gibbs free energy of OER/HER intermediates for overall water splitting. Materials Today Chemistry, 2022, 23, 100634.	1.7	58
25	Two-Dimensional Semiconducting Boron Monolayers. Journal of the American Chemical Society, 2017, 139, 17233-17236.	6.6	57
26	Subâ€3 nm Intermetallic Ordered Pt ₃ In Clusters for Oxygen Reduction Reaction. Advanced Science, 2020, 7, 1901279.	5.6	57
27	CoSe2 modified Se-decorated CdS nanowire Schottky heterojunctions for highly efficient photocatalytic hydrogen evolution. Chemical Engineering Journal, 2020, 389, 124431.	6.6	57
28	Selective on-surface covalent coupling based on metal-organic coordination template. Nature Communications, 2019, 10, 70.	5.8	55
29	Stabilizing forces acting on ZnO polar surfaces: STM, LEED, and DFT. Physical Review B, 2014, 89, .	1.1	54
30	Recipe for Dirac Phonon States with a Quantized Valley Berry Phase in Two-Dimensional Hexagonal Lattices. Nano Letters, 2018, 18, 7755-7760.	4.5	54
31	Ideal type-III nodal-ring phonons. Physical Review B, 2020, 101, .	1.1	53
32	Hydrogen and oxygen adsorption on ZnO nanowires: A first-principles study. Physical Review B, 2009, 79, .	1.1	51
33	ldeal intersecting nodal-ring phonons in bcc <mml:math xmlns:mml="http://www.w3.org/1998/Math/MathML"><mml:msub><mml:mi mathvariant="normal">C<mml:mn>8</mml:mn></mml:mi </mml:msub>. Physical Review B, 2018. 98</mml:math 	1.1	51
34	Properties of rare-earth iron garnets from first principles. Physical Review B, 2017, 95, .	1.1	50
35	Ferromagnetic Weyl semimetal phase in a tetragonal structure. Physical Review B, 2017, 96, .	1.1	48
36	A (001) dominated conjugated polymer with high-performance of hydrogen evolution under solar light irradiation. Chemical Communications, 2017, 53, 10536-10539.	2.2	47

#	Article	IF	CITATIONS
37	Quantum Effects and Phase Tuning in Epitaxial Hexagonal and Monoclinic MoTe ₂ Monolayers. ACS Nano, 2017, 11, 3282-3288.	7.3	46
38	Splitting Water on Metal Oxide Surfaces. Journal of Physical Chemistry C, 2011, 115, 19710-19715.	1.5	45
39	A novel 2D Co3(HADQ)2 metal-organic framework as a highly active and stable electrocatalyst for acidic oxygen reduction. Chemical Engineering Journal, 2022, 430, 132642.	6.6	43
40	Onâ€surface Synthesis of a Semiconducting 2D Metal–Organic Framework Cu ₃ (C ₆ O ₆) Exhibiting Dispersive Electronic Bands. Angewandte Chemie - International Edition, 2020, 59, 2669-2673.	7.2	42
41	Density-functional theory calculations of bare and passivated triangular-shaped ZnO nanowires. Applied Physics Letters, 2007, 91, 031914.	1.5	41
42	Dual Defectâ€Passivation Using Phthalocyanine for Enhanced Efficiency and Stability of Perovskite Solar Cells. Small, 2021, 17, e2005216.	5.2	40
43	New approaches for calculating absolute surface energies of wurtzite (0001)/(0001Â ⁻): A study of ZnO and GaN. Journal of Applied Physics, 2016, 119, .	1.1	39
44	Phonon-mediated superconductivity in Mg intercalated bilayer borophenes. Physical Chemistry Chemical Physics, 2017, 19, 29237-29243.	1.3	39
45	Two-Dimensional Metal-Phosphorus Network. Matter, 2020, 2, 111-118.	5.0	39
46	Antibacterial and photocatalytic activity of TiO2 and ZnO nanomaterials in phosphate buffer and saline solution. Applied Microbiology and Biotechnology, 2013, 97, 5565-5573.	1.7	38
47	Unraveling the oxide layer on Mo2C as the active center for hydrogen evolution reaction. Journal of Catalysis, 2020, 389, 461-467.	3.1	38
48	Synthesis and characterization of a single-layer conjugated metal–organic structure featuring a non-trivial topological gap. Nanoscale, 2019, 11, 878-881.	2.8	37
49	Symmetry-enforced straight nodal-line phonons. Physical Review B, 2021, 104, .	1.1	37
50	Anchoring an Fe Dimer on Nitrogen-Doped Graphene toward Highly Efficient Electrocatalytic Ammonia Synthesis. ACS Applied Materials & Interfaces, 2021, 13, 43632-43640.	4.0	37
51	New Family of Two-Dimensional Ternary Photoelectric Materials. ACS Applied Materials & Interfaces, 2019, 11, 14457-14462.	4.0	35
52	Ideal Nodal Line Semimetal in a Two-Dimensional Boron Bilayer. Journal of Physical Chemistry C, 2019, 123, 4977-4983.	1.5	35
53	Tuning Electronic Structures of ZnO Nanowires by Surface Functionalization: A First-Principles Study. Journal of Physical Chemistry C, 2010, 114, 8861-8866.	1.5	34
54	Accelerating CO2 reduction on novel double perovskite oxide with sulfur, carbon incorporation: Synergistic electronic and chemical engineering. Chemical Engineering Journal, 2022, 446, 137161.	6.6	34

#	Article	IF	CITATIONS
55	Two-Dimensional Li-Based Ternary Chalcogenides for Photocatalysis. Journal of Physical Chemistry Letters, 2019, 10, 6061-6066.	2.1	31
56	Mechanically-Controlled Reversible Spin Crossover of Single Fe-Porphyrin Molecules. ACS Nano, 2017, 11, 6295-6300.	7.3	29
57	Three-terminal Weyl complex with double surface arcs in a cubic lattice. Npj Computational Materials, 2020, 6, .	3.5	29
58	Hybridization-induced gapped and gapless states on the surface of magnetic topological insulators. Physical Review B, 2020, 102, .	1.1	29
59	Surface Defects-Induced p-type Conduction of Silicon Nanowires. Journal of Physical Chemistry C, 2011, 115, 18453-18458.	1.5	28
60	Absolute determination of optical constants by reflection electron energy loss spectroscopy. Physical Review B, 2017, 95, .	1.1	28
61	Versatile and Highly Efficient Controls of Reversible Topotactic Metal–Insulator Transitions through Proton Intercalation. Advanced Functional Materials, 2019, 29, 1907072.	7.8	28
62	Reformation of thiophene-functionalized phthalocyanine isomers for defect passivation to achieve stable and efficient perovskite solar cells. Journal of Energy Chemistry, 2022, 67, 263-275.	7.1	28
63	Quantum Confined Tomonaga–Luttinger Liquid in Mo ₆ Se ₆ Nanowires Converted from an Epitaxial MoSe ₂ Monolayer. Nano Letters, 2020, 20, 2094-2099.	4.5	27
64	Three-dimensional quantum anomalous Hall effect in ferromagnetic insulators. Physical Review B, 2018, 98, .	1.1	25
65	Multiphotoluminescence from a Triphenylamine Derivative and Its Application in White Organic Lightâ€Emitting Diodes Based on a Single Emissive Layer. Advanced Materials, 2019, 31, e1900613.	11.1	25
66	Nodal line fermions in magnetic oxides. Physical Review B, 2018, 97, .	1.1	24
67	The synchronous improvement of strength and plasticity (SISP) in new Ni-Co based disc superalloys by controling stacking fault energy. Scientific Reports, 2017, 7, 8046.	1.6	23
68	Highly Degenerate Ground States in a Frustrated Antiferromagnetic Kagome Lattice in a Two-Dimensional Metal–Organic Framework. Journal of Physical Chemistry Letters, 2021, 12, 3733-3739.	2.1	23
69	Porous aza-doped graphene-analogous 2D material a unique catalyst for CO2 conversion to formic-acid by hydrogenation and electroreduction approaches. Molecular Catalysis, 2022, 524, 112285.	1.0	23
70	N-doped ZnO nanowires: Surface segregation, the effect of hydrogen passivation and applications in spintronics. Physica Status Solidi (B): Basic Research, 2010, 247, 2195-2201.	0.7	22
71	Highly efficient H2 generation over Cu2Se decorated CdS0.95Se0.05 nanowires by photocatalytic water reduction. Chemical Engineering Journal, 2021, 409, 128157.	6.6	22
72	Tunable double Weyl phonons driven by chiral point group symmetry. Physical Review B, 2021, 103, .	1.1	22

#	Articleion of <mml:math <br="" xmlns:mml="http://www.w3.org/1998/Math/MathML">display="inline"><mml:mrow><mml:msub><mml:mtext>O</mml:mtext><mml:mn>2</mml:mn></mml:msub></mml:mrow></mml:math>	IF /mml·mrow	CITATIONS
73	xmlns:mml="http://www.w3.org/1998/Math/MathML" display="inline"> <mml:mrow><mml:msub><mml:mtext>H</mml:mtext><mml:mn>2</mml:mn></mml:msub> xmlns:mml="http://www.w3.org/1998/Math/MathML"</mml:mrow>		
74	Controlling the Reaction Steps of Bifunctional Molecules 1,5-Dibromo-2,6-dimethylnaphthalene on Different Substrates. Journal of Physical Chemistry C, 2018, 122, 13001-13008.	1.5	21
75	Charge Density Modulation and the Luttinger Liquid State in MoSe ₂ Mirror Twin Boundaries. ACS Nano, 2020, 14, 10716-10722.	7.3	21
76	First-principles study of the size-dependent structural and electronic properties of thick-walled ZnO nanotubes. Solid State Communications, 2008, 148, 534-537.	0.9	20
77	Ferromagnetic Weyl fermions in CrO2. Physical Review B, 2018, 97, .	1.1	20
78	Surface Adsorption and Vacancy in Tuning the Properties of Tellurene. ACS Applied Materials & Interfaces, 2020, 12, 19110-19115.	4.0	20
79	Strain-induced water dissociation on supported ultrathin oxide films. Scientific Reports, 2016, 6, 22853.	1.6	19
80	Size-, electric-field- and frequency-dependent third-order nonlinear optical properties of hydrogenated silicon nanoclusters. Scientific Reports, 2016, 6, 28067.	1.6	19
81	Emergence of topological nodal loops in alkaline-earth hexaborides XB ₆ (X = Ca, Sr, and) Tj ETQq1	1 0.784314 1.3	rgßt /Over
82	Oxidation-Induced Topological Phase Transition in Monolayer 1T′-WTe ₂ . Journal of Physical Chemistry Letters, 2018, 9, 4783-4788.	2.1	19
83	An electron compensation mechanism for the polymorphism of boron monolayers. Nanoscale, 2018, 10, 13410-13416.	2.8	19
84	Two-Dimensional Dirac Semimetals without Inversion Symmetry. Physical Review Letters, 2020, 125, 116402.	2.9	19
85	Interaction of O2 with reduced rutile TiO2(110) surface. Surface Science, 2013, 610, 33-41.	0.8	18
86	Large-gap quantum anomalous Hall phase in hexagonal organometallic frameworks. Physical Review B, 2018, 98, .	1.1	18
87	The Enhancement of Surface Reactivity on CeO ₂ (111) Mediated by Subsurface Oxygen Vacancies. Journal of Physical Chemistry C, 2016, 120, 27917-27924.	1.5	17
88	Role of surface adsorption in tuning the properties of black phosphorus. Physical Chemistry Chemical Physics, 2018, 20, 112-117.	1.3	17
89	Extremely High Mobilities in Two-Dimensional Group-VA Binary Compounds with Large Conversion Efficiency for Solar Cells. Journal of Physical Chemistry C, 2018, 122, 27590-27596.	1.5	17
90	Intrinsic Ferromagnetic Semiconductors in Two-Dimensional Alkali-Based Chromium Chalcogenides. ACS Applied Electronic Materials, 2020, 2, 3853-3858.	2.0	17

#	ARTICLE	IF	CITATIONS
91	Hybrid nodal-ring phonons with hourglass dispersion in <mml:math xmlns:mml="http://www.w3.org/1998/Math/MathML"><mml:msub><mml:mi>AgAlO</mml:mi><mml:mn>2Physical Review Materials, 2022, 6, .</mml:mn></mml:msub></mml:math 	ml :ឈ 9> <td>mml:7nsub>«/</td>	mm l:7 nsub>«/
92	Hole doping in epitaxial MoSe ₂ monolayer by nitrogen plasma treatment. 2D Materials, 2018, 5, 041005.	2.0	16
93	A Shallow Acceptor of Phosphorous Doped in MoSe ₂ Monolayer. Advanced Electronic Materials, 2020, 6, 1900830.	2.6	16
94	Strain-tunable out-of-plane polarization in two-dimensional materials. Physical Review B, 2020, 101, .	1.1	16
95	Realizing graphene-like Dirac cones in triangular boron sheets by chemical functionalization. Journal of Materials Chemistry C, 2020, 8, 2798-2805.	2.7	16
96	Comparative optical study of colloidal anatase titania nanorods and atomically thin wires. Nanoscale, 2013, 5, 1465.	2.8	15
97	Generation of highly reactive oxygen species on metal-supported MgO(100) thin films. Physical Chemistry Chemical Physics, 2016, 18, 25373-25379.	1.3	15
98	Unusual dissociative adsorption of H2 over stoichiometric MgO thin film supported on molybdenum. Applied Surface Science, 2016, 366, 166-172.	3.1	15
99	Tunable ferromagnetic Weyl fermions from a hybrid nodal ring. Npj Computational Materials, 2019, 5, .	3.5	15
100	Developing Proton-Conductive Metal Coordination Polymer as Highly Efficient Electrocatalyst toward Oxygen Reduction. Journal of Physical Chemistry Letters, 2021, 12, 9197-9204.	2.1	15
101	Direct Z-scheme MoSe2/TiO2 heterostructure with improved piezoelectric and piezo-photocatalytic performance. Journal of Colloid and Interface Science, 2022, 622, 637-651.	5.0	15
102	An energetic stability predictor of hydrogen-terminated Si nanostructures. Applied Physics Letters, 2009, 95, .	1.5	14
103	Identifying Multinuclear Organometallic Intermediates in Onâ€Surface [2+2] Cycloaddition Reactions. Angewandte Chemie - International Edition, 2019, 58, 16485-16489.	7.2	14
104	Robust Twin Pairs of Weyl Fermions in Ferromagnetic Oxides. Physical Review Letters, 2019, 122, 057205.	2.9	14
105	Classification and materials realization of topologically robust nodal ring phonons. Physical Review Materials, 2021, 5, .	0.9	14
106	Metal-organic framework-derived three-dimensional CoSe2/Cd0.8Zn0.2S Schottky junction for highly efficient photocatalytic H2 evolution. Applied Surface Science, 2022, 593, 153420.	3.1	14
107	Ground states of group-IV nanostructures: Magic structures of diamond and silicon nanocrystals. Physical Review B, 2011, 83, .	1.1	13
108	The characteristics of flocs and zeta potential in nano-TiO2 system under different coagulation conditions. Colloids and Surfaces A: Physicochemical and Engineering Aspects, 2014, 452, 181-188.	2.3	13

#	Article	IF	CITATIONS
109	A Practical Criterion for Screening Stable Boron Nanostructures. Journal of Physical Chemistry C, 2017, 121, 11950-11955.	1.5	13
110	Stabilizing and Organizing Bi ₃ Cu ₄ and Bi ₇ Cu ₁₂ Nanoclusters in Twoâ€Dimensional Metal–Organic Networks. Angewandte Chemie - International Edition, 2018, 57, 4617-4621.	7.2	12
111	Intrinsic Role of Excess Electrons in Surface Reactions on Rutile TiO ₂ (110): Using Water and Oxygen as Probes. Journal of Physical Chemistry C, 2018, 122, 8270-8276.	1.5	12
112	NiSe ₂ as Co atalyst with CdS: Nanocomposites for Highâ€Performance Photodriven Hydrogen Evolution under Visible‣ight Irradiation. ChemPlusChem, 2019, 84, 999-1010.	1.3	12
113	The effect of DMPO on the formation of hydroxyl radicals on the rutile TiO ₂ (110) surface. Physical Chemistry Chemical Physics, 2020, 22, 13129-13135.	1.3	12
114	First-Principles Study of the Structural Stability and Electronic Properties of ZnS Nanowires. Journal of Physical Chemistry C, 2008, 112, 20291-20294.	1.5	11
115	Theoretical investigation of structural stability and electronic properties of hydrogenated silicon nanocrystals: Size, shape, and surface reconstruction. Physical Review B, 2012, 86, .	1.1	11
116	High Reactivity of the ZnO(0001) Polar Surface: The Role of Oxygen Adatoms. Journal of Physical Chemistry C, 2017, 121, 15711-15718.	1.5	11
117	Symmetry-Assisted Protection and Compensation of Hidden Spin Polarization in Centrosymmetric Systems. Chinese Physics Letters, 2020, 37, 087105.	1.3	11
118	Avoiding Sabatier's conflict in bifunctional heterogeneous catalysts for the WGS reaction. CheM, 2021, 7, 1271-1283.	5.8	11
119	Stability and Catalytic Performance of Singleâ€Atom Supported on Ti ₂ CO ₂ for Lowâ€Temperature CO Oxidation: A Firstâ€Principles Study. ChemPhysChem, 2021, 22, 2352-2361.	1.0	11
120	Anion Size Effect of Ionic Liquids in Tuning the Thermoelectric and Mechanical Properties of PEDOT:PSS Films through a Counterion Exchange Strategy. ACS Applied Materials & Interfaces, 2022, 14, 27911-27921.	4.0	11
121	Comment on "Interplay between Water andTiO2Anatase (101) Surface with Subsurface Oxygen Vacancy― Physical Review Letters, 2015, 115, 149601.	2.9	10
122	Splitting methanol on ultra-thin MgO(100) films deposited on a Mo substrate. Physical Chemistry Chemical Physics, 2017, 19, 7245-7251.	1.3	10
123	Remarkably Strong Chemisorption of Nitric Oxide on Insulating Oxide Films Promoted by Hybrid Structure. Journal of Physical Chemistry C, 2017, 121, 21482-21490.	1.5	10
124	First-principles study on the initial decomposition process of CH3NH3PbI3. Journal of Chemical Physics, 2017, 147, 124702.	1.2	10
125	Controllable dissociation of H ₂ O on a CeO ₂ (111) surface. Physical Chemistry Chemical Physics, 2018, 20, 1575-1582.	1.3	10
126	Adsorption Induced Indirect-to-Direct Band Gap Transition in Monolayer Blue Phosphorus. Journal of Physical Chemistry C, 2018, 122, 15792-15798.	1.5	10

#	Article	IF	CITATIONS
127	On-Surface Cascade Reaction Based on Successive Debromination via Metal–Organic Coordination Template. Langmuir, 2020, 36, 6286-6291.	1.6	10
128	Observation and Analysis of Ordered and Disordered Structures on the ZnO(0001) Polar Surface. Journal of Physical Chemistry C, 2016, 120, 26915-26921.	1.5	9
129	High-coverage stable structures of 3d transition metal intercalated bilayer graphene. Physical Chemistry Chemical Physics, 2016, 18, 14244-14251.	1.3	9
130	Heterolytic dissociative adsorption state of dihydrogen favored by interfacial defects. Applied Surface Science, 2018, 433, 862-868.	3.1	9
131	Single-layer Mo ₅ Te ₈ ― A new polymorph of layered transition-metal chalcogenide. 2D Materials, 2021, 8, 015006.	2.0	9
132	Stabilizing and activating dopants in ⟠112⟩ silicon nanowires by alkene adsorptions: A first-principles study. Applied Physics Letters, 2011, 98, 073115.	1.5	8
133	Dirac fermions in the antiferromagnetic spintronics material CuMnAs. Physical Review B, 2020, 102, .	1.1	8
134	Surface Passivationâ€Induced Strong Ferromagnetism of Zinc Oxide Nanowires. Chemistry - A European Journal, 2010, 16, 13072-13076.	1.7	7
135	Firstâ€principles calculations of atomic and electronic properties of ZnO nanostructures. Physica Status Solidi (B): Basic Research, 2010, 247, 2581-2593.	0.7	7
136	Controllable dissociations of PH ₃ molecules on Si(001). Nanotechnology, 2016, 27, 135704.	1.3	7
137	Stable sandwich structures of two-dimensional iron borides FeB _x alloy: a first-principles calculation. RSC Advances, 2017, 7, 30320-30326.	1.7	7
138	Surfaceâ€Dependent Chemoselectivity in Câ^'C Coupling Reactions. Angewandte Chemie - International Edition, 2019, 58, 8356-8361.	7.2	7
139	Robust Topological States in Bi ₂ Se ₃ against Surface Oxidation. Journal of Physical Chemistry C, 2020, 124, 6253-6259.	1.5	7
140	All-boron planar ferromagnetic structures: from clusters to monolayers. Nanoscale, 2021, 13, 9881-9887.	2.8	7
141	Unconventional line defects engineering in two-dimensional boron monolayers. Physical Review Materials, 2021, 5, .	0.9	7
142	Substrate mediated stabilization of methylphosphonic acid on ZnO non-polar surfaces'. Surface Science, 2012, 606, 289-292.	0.8	6
143	Recipe for generating Weyl semimetals with extended topologically protected features. Physical Review B, 2017, 96, .	1.1	6
144	Tunable magnetism in the LaAlO 3 /SrTiO 3 heterostructure: Insights from first-principles calculations. Physica E: Low-Dimensional Systems and Nanostructures, 2018, 98, 120-124.	1.3	6

#	Article	IF	CITATIONS
145	Kinetically Controlled Synthesis of Four―and Sixâ€Member Cyclic Products via Sequential Arylâ€Aryl Coupling on a Au(111) Surface. ChemPhysChem, 2019, 20, 2292-2296.	1.0	6
146	Type-II quadratic and cubic Weyl fermions. Physical Review B, 2022, 105, .	1.1	6
147	Metal-phosphorus network on Pt(111). 2D Materials, 2022, 9, 045002.	2.0	6
148	Atomic force microscopy study of small-size nanotubular polymer thin films. Journal of Materials Research, 1999, 14, 1084-1090.	1.2	5
149	Investigation on In Situ Tensile Behavior of Superalloy Bicrystals with Different CB Misorientations. Metallurgical and Materials Transactions A: Physical Metallurgy and Materials Science, 2014, 45, 3876-3881.	1.1	5
150	Quasi-One-Dimensional Metal-Insulator Transitions in Compound Semiconductor Surfaces. Physical Review Letters, 2016, 117, 116101.	2.9	5
151	The role of boundary conditions in tuning the electronic properties of the (0â€ ⁻ 0â€ ⁻ 1) LaAlO3/SrTiO3 interface. Computational Materials Science, 2018, 149, 354-359.	1.4	5
152	High Anisotropic Optoelectronics in Two Dimensional Layered PbSnX ₂ (X = S/Se). Journal of Physical Chemistry Letters, 2021, 12, 10574-10580.	2.1	5
153	Zhao etÂal. Reply. Physical Review Letters, 2017, 118, 239602.	2.9	4
154	Turning copper metal into a Weyl semimetal. Physical Review B, 2018, 97, .	1.1	4
155	Identifying Multinuclear Organometallic Intermediates in Onâ€6urface [2+2] Cycloaddition Reactions. Angewandte Chemie, 2019, 131, 16637-16641.	1.6	4
156	Topological Quantum States in Magnetic Oxides. Journal of Physical Chemistry Letters, 2020, 11, 4036-4042.	2.1	4
157	Structural Evolution and Underlying Mechanism of Single-Atom Centers on Mo2C(100) Support during Oxygen Reduction Reaction. ACS Applied Materials & Interfaces, 2021, 13, 17075-17084.	4.0	4
158	Giant magnetoresistance effect due to the tunneling between quantum anomalous Hall edge states. Applied Physics Letters, 2021, 118, .	1.5	4
159	New Family of Two-Dimensional Group-(II ₃ –V ₂) Photoelectric Materials. Journal of Physical Chemistry C, 2019, 123, 16851-16856.	1.5	3
160	Insights into the unusual semiconducting behavior in low-dimensional boron. Nanoscale, 2019, 11, 7866-7874.	2.8	3
161	Identification of electronic descriptors for catalytic activity of transition-metal and non-metal doped MoS ₂ . Physical Chemistry Chemical Physics, 2021, 23, 15101-15106.	1.3	3
162	Prominently enhanced corrosive gas NO2 resistibility for silicone rubber composite coatings by incorporation of functional g-C3N4 nanosheets. Progress in Organic Coatings, 2021, 157, 106292.	1.9	3

#	Article	IF	CITATIONS
163	Holes as Catalysts for CO Photo-Oxidation on Rutile TiO ₂ (110). Journal of Physical Chemistry C, 2022, 126, 6564-6569.	1.5	3
164	Straightforward strategy for selecting and tuning substrates for two-dimensional material epitaxy. Physical Review Materials, 2022, 6, .	0.9	3
165	Quantitative characterization of toughening mechanisms of rubber modified polymers. Science in China Series B: Chemistry, 1997, 40, 146-151.	0.8	2
166	Theoretical studies of geometry asymmetry in tellurium nanostructures: intrinsic dipole, charge separation, and semiconductor–metal transition. RSC Advances, 2014, 4, 44004-44010.	1.7	2
167	Surface reactivity enhancement by O2 dissociation on a single-layer MgO film deposited on metal substrate. Journal of Chemical Physics, 2016, 145, 164701.	1.2	2
168	Evidence of Weyl fermions in <mml:math xmlns:mml="http://www.w3.org/1998/Math/MathML"><mml:mrow><mml:mi>α</mml:mi><mml:mtext>â^²Physical Review B, 2021, 103, .</mml:mtext></mml:mrow></mml:math 	nl:mutext><	m æ ll:mi>Ru </td
169	Weyl fermions in ferromagnetic high-temperature phase of K ₂ Cr ₈ O ₁₆ . New Journal of Physics, 2020, 22, 073062.	1.2	2
170	Asymmetric valley polarization and photoluminescence in MoS ₂ /MoO ₃ heterostructure. Optics Express, 2019, 27, 38451.	1.7	2
171	Electrically modulated anomalous phase shift in Andreev bound states mediated by chiral Majorana modes. Physical Review B, 2022, 105, .	1.1	2
172	First-principles study of silicon bulk and nanowire (111) surfaces terminated with trihydrides: Symmetric, rotated, and tilted. Physical Review B, 2009, 80, .	1.1	1
173	Topological Rashba-like edge states in large-gap quantum spin Hall insulators. Physical Review Materials, 2018, 2, .	0.9	1
174	Theoretical studies of the passivants' effect on the SixGe1-x nanowires: Composition profiles, diameter, shape, and electronic properties. Journal of Chemical Physics, 2013, 139, 154713.	1.2	0